# 12 Interplay of Kondo Effect and RKKY Interaction

Johann Kroha
Physikalisches Institut, Universität Bonn
Nussallee 12, 53115 Bonn

## Contents



E. Pavarini, E. Koch, R. Scalettar, and R. Martin (eds.)
The Physics of Correlated Insulators, Metals, and Superconductors
Modeling and Simulation Vol. 7
Forschungszentrum Jülich, 2017, ISBN 978-3-95806-224-5
http://www.cond-mat.de/events/correl17

# 1 Introduction and overview

Magnetic interactions in a metal involving localized magnetic moments give rise to a wealth of phenomena, ranging from the Kondo effect to magnetic ordering and quantum phase transitions. We give a brief overview of such phenomena before, in the main part of these lecture notes, we will focus on a detailed description of the interplay of interactions that tend to quench the local moments or that tend order them.

When a magnetic ion is placed in a metallic host, the Kondo effect [1, 2] occurs: Conduction electrons at the Fermi level, i.e., at zero excitation energy, are in resonance with a flip of the two-fold degenerate spin ground state of the magnetic ion. As the temperature $T$ is lowered, the electrons become confined to the Fermi surface, so that more and more electrons contribute to this resonant quantum spin-flip scattering, leading to a diverging spin scattering amplitude. Hence, when the spin exchange coupling $J_0$ between the localized moments and the itinerant conduction electrons is antiferromagnetic, a many-body spin-singlet state between the impurity spin and the conduction electron spins is formed below a characteristic temperature, the Kondo temperature $T_K$. This, however, means that electrons that do not contribute to the singlet bound state, experience merely potential scattering rather than spin scattering, i.e., the impurity spin is effectively removed from the system. This effect is called spin screening. The scattering rate and other physical quantities thus settle smoothly to constant values, leading to Fermi-liquid behavior for $T \ll T_K$ [2]. The Kondo temperature is found to be exponentially small in the exchange coupling, $T_K = D_0 \exp[-1/(2N(0)J_0)]$, with the density of states at the Fermi level $N(0)$ and the conduction band width $D_0$. The entirety of complex phenomena sketched above, involving the increase of the spin scattering amplitude implying anomalous transport properties, followed by spin screening and the formation of a narrow, but smooth resonance of width $T_K$ in the electronic spectrum at the Fermi energy, comprises the Kondo effect.

When there are several or many localized magnetic moments in a metal, for instance arranged on a lattice, the same spin-exchange coupling $J_0$ that induces the Kondo effect, induces also a magnetic interaction between the localized spins: The local moments can exchange their spins, mediated by two conduction electrons scattering from and traveling between the impurity sites. Since this effective, long-range spin-exchange coupling $K$ involves two elementary scattering events between electron and und impurity spins, it is of order $K \propto N(0)J_0^2$. It can be ferro- or antiferromagnetic due to the long-range, spatial oscillations of the conduction electron density correlations. This conduction-electron-mediated spin interaction was first considered by Ruderman and Kittel [3], Kasuya [4] and Yosida [5] and is therefore called RKKY interaction. The RKKY interaction usually dominates the magnetic dipole-dipole coupling as well as the direct exchange coupling between neighboring local moments because of the short spatial extent of these couplings or the exponentially small overlap of the local moment wave functions on neighboring lattice sites.

In a Kondo lattice, the local Kondo coupling and the RKKY interaction favor different ground states. The Kondo coupling leads to a paramagnetic Fermi liquid state without local moments. In this state, the local orbitals, whose spectrum has a Kondo resonance at the Fermi energy,

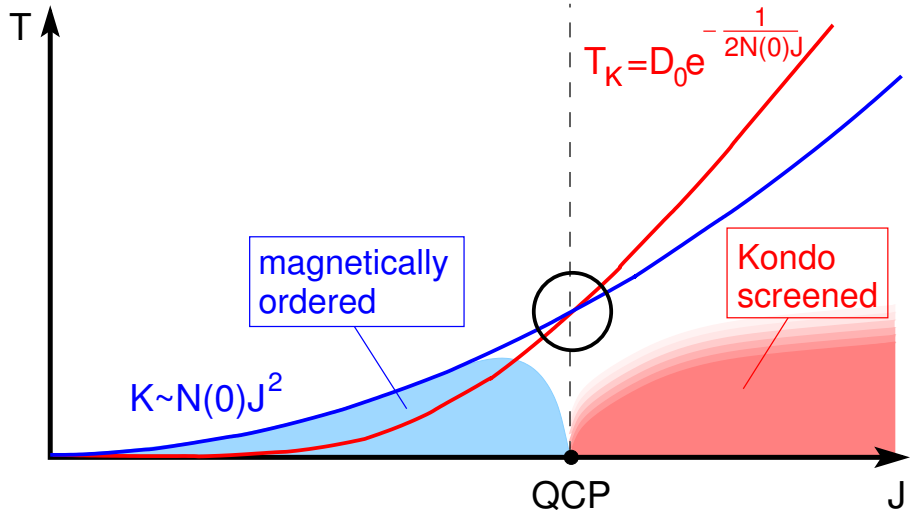


**Fig. 1:** *Doniach's phenomenological phase diagram for the phase transition between an RKKY-induced, magnetically ordered phase and the Kondo screened, paramagnetic phase. The phase transition occurs when the RKKY coupling $K$ of a local moment to all surrounding moments becomes equal to the Kondo singlet binding energy $T_K$ (black circle). While the RKKY coupling is $K \sim N(0)J_0^2$, the Kondo energy $T_K = D_0 \exp[-1/(2N(0)J_0)]$ is exponentially small in the bare, local spin exchange coupling $J$. Therefore, the RKKY coupling always dominates for small values of $J_0$.*

hybridize with each other and eventually become lattice coherent at low temperatures to form Bloch-like quasiparticle states. As a result, a narrow band crossing the Fermi energy is formed. Its bandwidth is controlled by the Kondo resonance width $T_K$. It thus gives rise to an exponentially strong effective mass enhancement of roughly $m^*/m \approx \exp[1/(2N(0)J_0)]$, which lends the name "heavy Fermi liquid" to this state [6].

By contrast, the RKKY interaction tends to induce magnetic order of the local moments. It was pointed out early on by Doniach [7] that, therefore, the Kondo spin screening of the local moments should eventually break down and give way to magnetic order, when the RKKY coupling energy becomes larger than the characteristic energy scale for Kondo singlet formation, the Kondo temperature $T_K$, see Fig. 1. Thus, one expects a $T = 0$ quantum phase transition (QPT) to occur [6], with the local spin exchange coupling $J_0$ as the control parameter. If and how the Kondo breakdown occurs at a magnetic QPT is, however, controversial. In fact, several QPT scenarios in heavy-fermion systems are conceivable.

(1) The heavy Fermi liquid, like any other Fermi liquid, may undergo a spin density-wave (SDW) instability, leading to critical fluctuations of the bosonic magnetic order parameter but leaving the fermionic, heavy quasiparticles intact. This scenario is well described by the pioneering works of Hertz, Moriya, and Millis [8–10].

(2) The local fluctuations of the magnetization, coupling to the nearly localized, heavy quasiparticles, may become critical (divergent) and thereby destroy the heavy Fermi liquid (local quantum criticality) [11, 12].

(3) At the phase transition the Kondo effect and, hence, the heavy-fermion band vanish, which leads to an abrupt change of the Fermi surface (Fermi volume collapse). It has been proposed [13] that the Fermi surface fluctuations associated with this change may self-consistently destroy the Kondo singlet state.
(4) Most recently, a scenario of critical quasiparticles has been put forward, characterized by a diverging effective mass and a singular quasiparticle interaction which is self-consistently generated by the nonlocal order-parameter fluctuations of an impending SDW instability [14–16]. Intriguing in its generality and similar in spirit to Landau's Fermi liquid theory, this scenario does, however, not invoke Kondo physics and, thus, does not address the specific problems associated with the Kondo destruction like Fermi volume collapse or the possibility of small, localized magnetic moments in the magnetically ordered phase.

While the Hertz-Millis-Moriya scenario (1) is described by a critical field theory of the bosonic, magnetic order parameter alone, the complete understanding of the breakdown scenarios (2), (3), and (4) would require a field theory for the fermionic degrees of freedom forming the Kondo effect and the heavy quasiparticles, coupled to the bosonic order parameter field. In lack of such a complete theory, these scenarios presume that specific fluctuations: (2) local fluctuations, (3) Fermi surface fluctuations, or (4) antiferromagnetic fluctuations, become soft for certain values of the system parameters and, thus, dominate the QPT. Therefore, the conditions for these scenarios to be realized are controversial.

In these lecture notes we consider the interplay of Kondo screening and RKKY interaction within the Kondo lattice model. We derive the phenomena of the single-impurity Kondo model in section 2, thereby introducing important concepts and techniques, like the fermionic representation spin, universality, and the analytic (perturbative) renormalization group. Section 3 presents the oscillatory RKKY coupling, calculated as a second-order spin exchange process, mediated by the conduction electrons. In section 4 we show how the Kondo singlet formation as well as the RKKY interaction can be incorporated on the same footing in an analytic renormalization group treatment, leading to a universal Kondo destruction as function of the RKKY coupling parameter. We conclude in section 5 with a discussion how this theory may set the stage for a more complete quantum field theory of heavy-fermion QPTs with Kondo breakdown.

# 2 Kondo effect and renormalization group

In this section we recollect the essential physics of a single Kondo impurity in a metal and provide the calculational tools for their derivation. We consider the single-impurity Kondo model

$$H = \sum_{\mathbf{k},\sigma} \varepsilon_{\mathbf{k}}\, c^\dagger_{\mathbf{k}\sigma} c_{\mathbf{k}\sigma} + J_0\, \hat{\mathbf{S}} \cdot \hat{\mathbf{s}} \tag{1}$$

where $c_{\mathbf{k}\sigma}$, $c^\dagger_{\mathbf{k}\sigma}$ denote the conduction ($c$-) electron operators with momentum $\mathbf{k}$ and dispersion $\varepsilon_{\mathbf{k}}$. $\hat{\mathbf{S}}$ is the impurity spin operator at site $\mathbf{x} = 0$, which is locally coupled to the spins of the

conduction electrons on that site, $\hat{\mathbf{s}}$, via a Heisenberg exchange coupling $J_0$. We have

$$\hat{\mathbf{s}} = \sum_{\mathbf{k},\mathbf{k}',\,\sigma,\sigma'} c^{\dagger}_{\mathbf{k}\sigma}\, \boldsymbol{\sigma}_{\sigma\sigma'}\, c_{\mathbf{k}'\sigma'}, \tag{2}$$

with $\boldsymbol{\sigma} = (\sigma_x,\, \sigma_y,\, \sigma_z)^T$ the vector of Pauli matrices

$$\sigma_x = \begin{pmatrix} 0 & 1 \\ 1 & 0 \end{pmatrix} \qquad \sigma_y = \begin{pmatrix} 0 & -i \\ i & 0 \end{pmatrix} \qquad \sigma_z = \begin{pmatrix} 1 & 0 \\ 0 & -1 \end{pmatrix}. \tag{3}$$

In Eq. (2) the conduction spin eigenvalue $1/2$ has been absorbed in the coupling constant $J_0$, by convention, and we use units $\hbar = 1$ throughout. The local spins $\hat{\mathbf{S}}$ will henceforth be termed $f$-spins, as they are typically realized in heavy fermion systems by the rare-earth $4f$ electrons.

## 2.1 Pseudo-fermion representation of spin

A field theoretical treatment, like the standard functional integral or Wick's theorem and many-body perturbation theory, requires that the corresponding field operators obey canonical commutation rules, i.e., their (anti)commutators must be proportional to the unit operator. However, the spin operators $\hat{\mathbf{S}}$ obey the SU(2) algebra. In order to overcome this difficulty, we use the fermionic representation of spin, first introduced by Abrikosov [17]. For each of the basis states spanning the impurity spin Hilbert space, $|\sigma\rangle$, $\sigma = \uparrow, \downarrow$, fermionic creation and destruction operators $f^{\dagger}_{\sigma}$, $f_{\sigma}$ are introduced according to $|\sigma\rangle = f^{\dagger}_{\sigma}|vac\rangle$, where $|vac\rangle$ denotes the vacuum state (no impurity spin present). The impurity spin operator $\mathbf{S}$ then reads,

$$\hat{\mathbf{S}} = \frac{1}{2} \sum_{\tau,\tau'} f^{\dagger}_{\tau}\, \boldsymbol{\sigma}_{\tau\tau'}\, f_{\tau'}. \tag{4}$$

That is, the operator on the right-hand side and $\hat{\mathbf{S}}$ have identical matrix elements in the physical spin Hilbert space. However, repeated action of the fermionic operators would permit unphysical double occupancy or no occupancy of the spin states $|\uparrow\rangle$, $|\downarrow\rangle$. The dynamics are restricted to the physical spin space by imposing the operator constraint

$$\hat{Q} = \sum_{\sigma} f^{\dagger}_{i\tau} f_{i\tau} = \mathbb{1}. \tag{5}$$

Eqs. (4), (5) constitute the exact pseudo-fermion representation of the spin $s = 1/2$.
The impurity-spin operator and, hence, the equation of motion with the Hamiltonian (1) are symmetric under the local U(1) gauge transformation

$$f_{\tau} \to \mathrm{e}^{-i\phi(t)} f_{\tau}, \qquad i\frac{d}{dt} \to i\frac{d}{dt} - \frac{\partial \phi(t)}{\partial t}, \tag{6}$$

with an arbitrary, time-dependent phase $\phi(t)$. It is closely related to the conservation of the pseudo-fermion number $\hat{Q}$.

*Projection onto the physical Hilbert space.* The exact projection of the dynamics onto the physical sector of Fock space with $Q = 1$, is performed by the following procedure. Consider first the grand canonical ensemble with respect to $Q$, defined by the statistical operator

$$\hat{\rho}_G = \frac{1}{Z_G} \mathrm{e}^{-\beta(H+\lambda Q)}, \tag{7}$$

where $Z_G = \mathrm{tr}[\exp\{-\beta(\hat{H} + \lambda\hat{Q})\}]$ is the grand canonical partition function, $-\lambda$ the associated chemical potential, and $\beta = 1/k_B T$ the inverse temperature. The trace extends over the complete Fock space, including summation over $Q =$ 0, 1, 2. The grand canonical expectation value of an observable $\hat{A}$ acting on the impurity spin space is defined as

$$\langle \hat{A} \rangle_G(\lambda) = \mathrm{tr}[\hat{\rho}_G \hat{A}]. \tag{8}$$

The physical expectation value of $\hat{A}$, $\langle \hat{A} \rangle$, must be evaluated in the canonical ensemble with fixed $Q = 1$. It can be obtained from the grand canonical expectation value as [17],

$$\langle \hat{A} \rangle := \frac{\mathrm{tr}_{Q=1}\left[\hat{A} e^{-\beta \hat{H}}\right]}{\mathrm{tr}_{Q=1}\left[e^{-\beta \hat{H}}\right]} = \lim_{\lambda\to\infty} \frac{\mathrm{tr}\left[\hat{A} e^{-\beta[\hat{H}+\lambda(\hat{Q}-1)]}\right]}{\mathrm{tr}\left[\hat{Q} e^{-\beta[\hat{H}+\lambda(\hat{Q}-1)]}\right]} = \lim_{\lambda\to\infty} \frac{\langle \hat{A} \rangle_G(\lambda)}{\langle \hat{Q} \rangle_G(\lambda)} \tag{9}$$

Here, all terms of the grand canonical traces in the numerator and in the denominator with $Q > 1$ are projected away by the limit $\lambda \to \infty$. In the denominator, the operator $\hat{Q}$ makes all terms with $Q = 0$ vanish. In the numerator, the observable $\hat{A}$ acts on the impurity spin space and hence is a power of $\hat{S}$, Eq. (4), which vanishes in the $Q = 0$ subspace. Therefore, in the numerator and in the denominator precisely the canonical traces over the physical sector $Q = 1$ remain, as required. It follows that any impurity-spin correlation function can be evaluated as a pseudo-fermion correlation function in the unrestricted Fock space, where Wick's theorem and the decomposition in terms of Feynman diagrams with pseudo-fermion propagators are valid, and taking the limit $\lambda \to \infty$ at the end of the calculation. Note that for the $c$ electron spin, Eq. (2), the $Q = 1$ projection is not needed, because for the noninteracting $c$-electrons doubly occupied or empty states are allowed.

*Diagrammatic rules.* We will now show that the limit $\lambda \to \infty$ translates into simple diagrammatic rules for the evaluation of impurity Green and correlation functions. We denote the local $c$ electron Green function at the impurity site by $G_{c\sigma}(i\omega_n)$ and the bare, grand canonical pseudo-fermion Green function by $G^G_{f\sigma}(i\omega_n)$

$$G_{c\sigma}(i\omega_n) = \sum_{\mathbf{k}} \frac{1}{i\omega_n - \varepsilon_{\mathbf{k}}} \tag{10}$$

$$G^G_{f\sigma}(i\omega_n) = \frac{1}{i\omega_n - \lambda}, \tag{11}$$

with the fermionic Matsubara frequencies $\omega_n = \frac{\pi}{\beta}(2n+1)$. Consider first $\lim_{\lambda\to 0}\langle \hat{Q} \rangle_G(\lambda)$. Using standard, complex contour integration, we obtain

$$\begin{aligned} \langle \hat{Q} \rangle_G(\lambda) &= \sum_\sigma \frac{1}{\beta} \sum_{\omega_n} G^G_{f\sigma}(i\omega_n) = -\sum_\sigma \oint \frac{dz}{2\pi i} f(z)\, G^G_{f\sigma}(z) \\ &= -\sum_\sigma \int_{-\infty}^{+\infty} \frac{d\varepsilon}{2\pi i} f(\varepsilon) \left[G^G_{f\sigma}(\varepsilon + i0) - G^G_{f\sigma}(\varepsilon - i0)\right], \end{aligned} \tag{12}$$

where $f(\varepsilon) = 1/(e^{\beta\varepsilon}+1)$ is the Fermi function, and the $\varepsilon$-integral extends along the branch cut of $G^G_{f\sigma}(z)$ at the real frequency axis, $\mathrm{Im}\, z = 0$. We can now perform a specific gauge transformation of the operators, $f_\tau \to \mathrm{e}^{-i\lambda t} f_\tau$. It implies, by virtue of Eq. (6), a shift of all pseudo-fermion energies in a diagram by $\varepsilon \to \varepsilon + \lambda$. It eliminates $\lambda$ from the pseudo-fermion propagator and casts it into the argument of the Fermi function. Thus, we have

$$\begin{aligned} \langle \hat{Q} \rangle_G(\lambda) &= -\sum_\sigma \int_{-\infty}^{+\infty} \frac{d\varepsilon}{\pi}\, f(\varepsilon+\lambda)\, \mathrm{Im}\, G_{f\sigma}(\varepsilon + i0) \\ &\stackrel{\lambda\to\infty}{\longrightarrow} \mathrm{e}^{-\beta\lambda} \sum_\sigma \int_{-\infty}^{+\infty} \frac{d\varepsilon}{\pi}\, \mathrm{e}^{-\beta\varepsilon}\, \mathrm{Im}\, G_{f\sigma}(\varepsilon + i0), \end{aligned} \tag{13}$$

where $G_{f\sigma}(\varepsilon + i0) \equiv G^G_{f\sigma}(\varepsilon + \lambda + i0) = 1/(\varepsilon + i0)$ is independent of $\lambda$.
The result Eq. (13) can be generalized by explicit calculation to arbitrary Feynman diagrams involving $f$- and $c$-Green functions: (i) Each complex contour integral includes one distribution function $f(z)$. The integral can be written as the sum of integrals along the branch cuts at the real energy axis of all propagators appearing in the diagram. (ii) Consider now one term of this sum. The argument of the distrubution function $f(\varepsilon)$ in that term is real and always equal to the argument $\varepsilon$ of that propagator $G$ along whose branch cut the integration extends. (iii) The above energy-shift gauge transformation applies to all pseudo-fermion energies $\omega$ in the diagram and, thus, cancels the parameter $\lambda$ in all pseudo-fermion propagators, $G^G_{f\sigma}(\omega) \to G_{f\sigma}(\omega)$. (iv) If in the considered term the integral is along a pseudo-fermion branch cut, this gauge transformation also shifts the argument of the distribution function, $f(\varepsilon) \to f(\varepsilon+\lambda)$, by virtue of (ii), i.e., the pseudo-fermion branch cut integral vanishes $\sim \mathrm{e}^{-\beta\lambda}$, as in Eq. (13). If the integral is along a $c$-electron branch cut, the argument of $f(\varepsilon)$ is not affected by the gauge transformation, and the integral does not vanish.
This derivation can be summarized in the following diagrammatic rules for ($Q = 1$)-projected expectation values:

(1) In a diagrammatic part that consists of a product of $c$- and $f$-Greens's functions, only the integrals along the $c$-electron branch cuts contribute.
(2) A closed pseudo-fermion loop contains only pseudo-fermion branch cut integrals and thus carries a factor $\mathrm{e}^{-\beta\lambda}$.
(3) Each diagram contributing to the projected expectation value of an impurity spin observable, $\langle \hat{A} \rangle$, contains exactly one closed pseudo-fermion loop per impurity site, because the factor of $\mathrm{e}^{-\beta\lambda}$ cancels in the numerator and denominator of Eq. (9), and higher order loops vanish by virtue of rule (2).

We note in passing that the pseudo-fermion representation can be generalized in a straightforward way to higher local spins than $S = 1/2$ by choosing in Eq. (4) a respective higher-dimensional representation of the spin matrices and defining the constraint $\hat{Q} = \mathbb{1}$ as before, with a summation over all possible spin orientations $\tau$. It can also be extended to include local charge fluctuations by means of the slave boson representation [18–21].

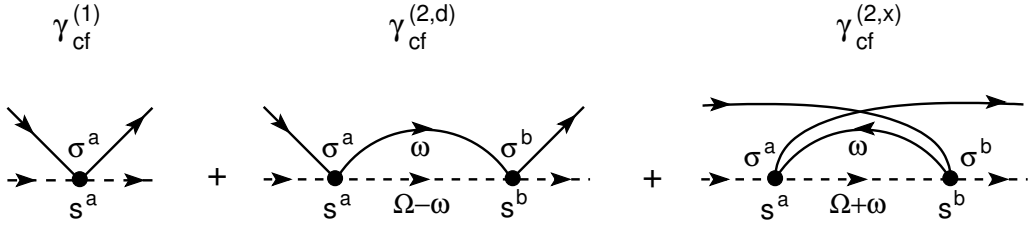


**Fig. 2:** *Conduction electron-impurity spin vertex $\hat{\gamma}_{cf}$ of the single-impurity Kondo model up to 2nd order in the spin exchange coupling $J_0$. Conduction electron propagators are denoted by solid, pseudo-fermion propagators by dashed lines. $\hat{\gamma}^{2,d}$ and $\hat{\gamma}^{2,x}$ represent the 2nd-order direct and exchange terms, respectively. The external lines are drawn for clarity and are not part of the vertex.*

## 2.2 Perturbation theory

It is instructive to analyze the scattering of a conduction electron from a spin impurity in perturbation theory, because this will visualize the physical origin of its singular behavior. The perturbation theory can be efficiently evaluated with the formalism developed in section 2.1.

With the Kondo Hamiltonian Eq. (1) the conduction-electron–impurity-spin vertex $\hat{\gamma}_{cf}$ can be read off from the diagrams in Fig. 2. Denoting the vector of Pauli matrices acting in $c$-electron spin space by $\boldsymbol{\sigma} = (\sigma^x, \sigma^y, \sigma^z)^T$ and the vector of Pauli matrices in $f$-spin space by $\mathbf{s} = (s^x, s^y, s^z)^T$, $\hat{\gamma}_{cf}$ reads in first and second order of $J_0$

$$\hat{\gamma}_{cf}^{(1)} = \frac{1}{2} J_0 \, (\mathbf{s} \cdot \boldsymbol{\sigma}) \tag{14}$$

$$\hat{\gamma}_{cf}^{(2,d)} = -\frac{1}{4} J_0^2 \sum_{a,b=x,y,z} \left(s^b \sigma^b\right) \left(s^a \sigma^a\right) \, \frac{1}{\beta} \sum_{\omega_n} G_c(i\omega_n) G_f(i\Omega_m - i\omega_n)|_{\lambda \to \infty} \tag{15}$$

$$\hat{\gamma}_{cf}^{(2,x)} = +\frac{1}{4} J_0^2 \sum_{a,b=x,y,z} \left(s^b \sigma^a\right) \left(s^a \sigma^b\right) \, \frac{1}{\beta} \sum_{\omega_n} G_c(i\omega_n) G_f(i\Omega_m + i\omega_n)|_{\lambda \to \infty}, \tag{16}$$

where matrix multiplications in the $f$- and $c$-spin spaces are implied, and the sum $\sum_{a=x,y,z}$ represents the scalar product in position space. The relative minus sign between $\hat{\gamma}_{cf}^{(2,d)}$ and $\hat{\gamma}_{cf}^{(2,x)}$ arises because of the extra fermion loop in the exchange term $\hat{\gamma}_{cf}^{(2,x)}$. Note that the order of the Pauli matrices in Eqs. (15), (16) is crucial. It is determined by their order along the $c$-electron or $f$-particle lines running through the diagram. Thus, in $\hat{\gamma}_{cf}^{(2,x)}$ the order of $c$-electron Pauli matrices is reversed with respect to $\hat{\gamma}_{cf}^{(2,d)}$.

The spin-dependent part of $\hat{\gamma}_{cf}^{(2,d)}$, $\hat{\gamma}_{cf}^{(2,x)}$ can be evaluated using the SU(2) spin algebra, $\sigma^a \sigma^b = \sum_{c=x,y,z} i\varepsilon^{abc}\sigma^c + \delta^{ab}\mathbb{1}$ for $a$, $b = x$, $y$, $z$, where $\mathbb{1}$ is the unit operator in spin space, $\varepsilon^{abc}$ the totally antisymmetric unit tensor and $\delta^{ab}$ the Kronecker-$\delta$

$$\mathrm{d}: \quad \sum_{a,b=x,y,z} s^b s^a \otimes \sigma^b \sigma^a = -2\,\mathbf{s}\cdot\boldsymbol{\sigma} + 3\,\mathbb{1}\otimes\mathbb{1} \tag{17}$$

$$\mathrm{x}: \quad \sum_{a,b=x,y,z} s^b s^a \otimes \sigma^a \sigma^b = 2\,\mathbf{s}\cdot\boldsymbol{\sigma} + 3\,\mathbb{1}\otimes\mathbb{1} \tag{18}$$

For scattering at the Fermi energy ($\Omega = 0$), the energy-dependent factors in Eqs. (15), (16) are

$$\begin{aligned} \mathrm{d}: \qquad \frac{1}{\beta}\sum_{\omega_n} G_c(i\omega_n)G_f^G(-i\omega_n)|_{\lambda\to\infty} &= \oint \frac{dz}{2\pi i}[1-f(z)]G_c(z)G_f^G(-z)|_{\lambda\to\infty} \\ &= N(0)\int_{-D_0}^{D_0} d\varepsilon\, \frac{1-f(\varepsilon)}{\varepsilon} \qquad (19) \\ \mathrm{x}: \qquad \frac{1}{\beta}\sum_{\omega_n} G_c(i\omega_n)G_f^G(i\omega_n)|_{\lambda\to\infty} &= -\oint \frac{dz}{2\pi i} f(z)G_c(z)G_f^G(z)|_{\lambda\to\infty} \\ &= -N(0)\int_{-D_0}^{D_0} d\varepsilon\, \frac{f(\varepsilon)}{\varepsilon}, \qquad (20) \end{aligned}$$

where we have assumed the Fermi energy in the center of the band of half bandwidth $D_0$, with a flat conduction electron density of states $N(0) = \mathrm{Im}\, G_c(0-i0)/\pi$. We see (cf. Fig. 2) that in the direct term ($d$) the intermediate electron must scatter into an unoccupied state, $1-f(\varepsilon)$, while in the exchange term ($x$) the intermediate electron comes from an occupied state, $f(\varepsilon)$ and then leaves the impurity. Collecting all terms, we obtain $\hat{\gamma}_{cf} = \hat{\gamma}_{cf}^{(1)} + \hat{\gamma}_{cf}^{(2d)} + \hat{\gamma}_{cf}^{(2x)}$ as

$$\begin{aligned} \hat{\gamma}_{cf} &= \frac{1}{2}J_0\,(\mathbf{s}\cdot\boldsymbol{\sigma})\,\left[1 + N(0)J_0\int_{-D_0}^{D_0} d\varepsilon\,\frac{1-2f(\varepsilon)}{\varepsilon} + \mathcal{O}(J_0^2)\right] \\ &\approx \frac{1}{2}J_0\,(\mathbf{s}\cdot\boldsymbol{\sigma})\,\left[1 + 2N(0)J_0\ln\left(\frac{D_0}{T}\right) + \mathcal{O}(J_0^2)\right] \qquad (21) \end{aligned}$$

The calculation clearly shows the physical origin of the logarithmic behavior: the presence of a sharp Fermi edge in the phase space available for scattering, i.e., in the integrals of Eqs. (19), (20), and quantum spin-flip scattering with the nontrivial SU(2) algebra. If the reversed order of Pauli matrices in the exchange term would not introduce a minus sign in the spin channel, Eq. (18), the logarithmic terms would cancel, like in the potential scattering channel, instead of adding up. It is also important that the impurity is localized, because otherwise an integral over the exchanged momentum (recoil) would smear the logarithmic singularity.

Eq. (21) exhibits a logarithmic divergence for low temperatures $T$. It signals a breakdown of perturbation theory when the 2nd-order contribution to $\hat{\gamma}_{cf}$ becomes equal to the 1st-order contribution. This happens at a characteristic temperature scale, which can be read off from Eq. (21), the Kondo temperature

$$T_K = D_0\,\mathrm{e}^{-1/(2N(0)J_0)}. \qquad (22)$$

Below $T_K$ perturbative calculations about the weak-coupling state break down. To describe the complex physics outlined in the introduction, more sophisticated techniques, predominantly numerical or exact solution methods, are required. The logarithmic behavior of the perturbation expansion, however, sets the stage for the development of the renormalization group method, to be developed in the next section, and which is particularly useful for analytically studying the interplay of Kondo screening and RKKY interaction.

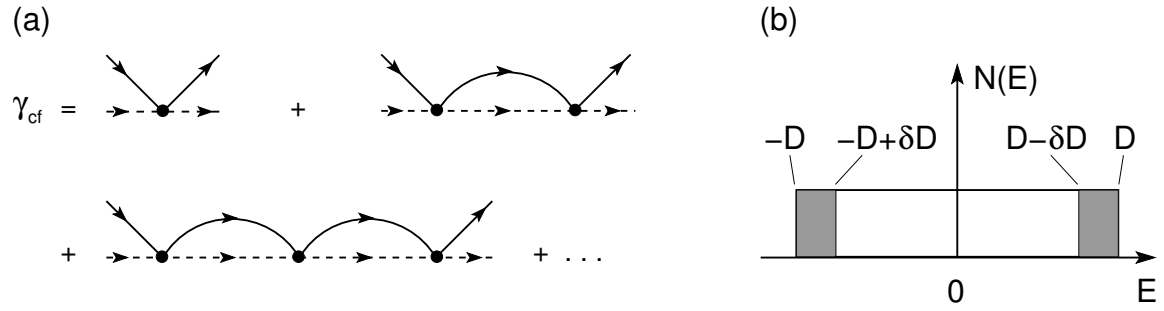


**Fig. 3:** *Universality and perturbative renormalization group. (a) T-matrix resummation of the $c$–$f$ vertex. The sum contains, for each conduction electron-pseudo-fermion bubble (direct diagram) shown, the exchange diagram, which is not shown for clarity. (b) Scheme for the cutoff reduction $D \to D - \delta D$.*

## 2.3 Renormalization group

Since the logarithm is a scale invariant function, there is the possibility that the resummation of a logarithmic perturbation expansion leads to universal behavior in the sense that variables like energy $\omega$, temperature $T$, etc. can be expressed in units of a single scale, $T_K$, in such a way that all physical quantities are functions of the dimensionless variables, $\omega/T_K$, $T/T_K$, etc. only and do not explicitly depend on the microscopic parameters of the Hamiltonian, like $J_0$, $D_0$, and $N(0)$. For the Kondo model, this extremely remarkable property can be visualized by a T-matrix-like, partial resummation of the $c$–$f$ vertex, as sketched in Fig. 3(a). The resummation results in a geometric series for the total $c$–$f$ vertex or the effective coupling constant $\tilde{J}$

$$N(0)\tilde{J} = 2N(0)J_0\left[1 + 2N(0)J_0\ln\left(\frac{D_0}{T}\right) + \left(2N(0)J_0\ln\left(\frac{D_0}{T}\right)\right)^2 + \ldots\right] \quad (23)$$

$$= \frac{2N(0)J_0}{1 - 2N(0)J_0\ln\left(\frac{D_0}{T}\right)} = \frac{1}{\ln\left(\frac{T}{T_K}\right)}, \quad (24)$$

which converges for $T > T_K$. It is seen that, as a consequence of the logarithmic behavior, in the last expression the microscopic parameters $J_0$, $D_0$, and $N(0)$ indeed conspire to form the Kondo temperature $T_K$ of Eq. (22) as the only scale in the problem. This universal behavior is inherited by physical quantities, like relaxation rates, transport properties, etc., since they can be expressed in terms of the total $c$–$f$ vertex. Although the above is only a heuristic argument and other contributions, not contained in the partial summation, could break the universality, it has been shown independently by the Bethe ansatz solution [22] and by numerical renormalization group (NRG) (for a recent review see [23]) that universality in the above sense indeed holds for the Kondo problem.

Universality is the starting point for the renormalization group method whose essence we discuss next. Let all physical quantities $A_n = h_n(\omega/T^*, T/T^*)$ of a system depend on energy $\omega$ and temperature $T$ in a universal way, with universal functions $h_n$ and some (yet unknown) characteristic scale $T^*$, which depends on the microscopic parameters of the Hamiltonian, $J_0$, $D_0$, $N(0)$. The fact that the $A_n$ depend on these parameters only implicitly through $T^*$

implies that different values of this parameter set realize the same physical system (defined by its observables $A_n$) if only the different parameter set values lead to the same scale $T^*$. In particular, systems with low and with high values of the conduction bandwidth or cutoff $D_0$ must be equivalent if the coupling constant $J_0$ is adjusted appropriately. In the Kondo problem we are mostly interested in the low-energy behavior, where the perturbation theory fails. This regime corresponds to electrons with a low bandwidth, scattering near the Fermi energy. By virtue of the above argument, this low-energy regime is connected with the high bandwidth regime, where perturbative calculations are possible. In the renormalization group method, this relation is established iteratively. Starting from an initial high-energy cutoff $D_0$, the cutoff is stepwise reduced to low energies, calculating at each step how the coupling constant $J$ of the Hamiltonian must be changed, such that the physical observables $A_n$ remain constant, see Fig. 3(b). This defines a running cutoff $D$ with initial value $D_0$ and a "renormalized" or "running" coupling constant $J(D)$ with initial value $J_0$. The running coupling constant, as part of the Hamiltonian, defines a change of the Hamiltonian itself. More generally, the cutoff reduction may even generate new types of interaction operators in the Hamiltonian, implied by the requirement that physical observables be invariant. The repeated operations on the Hamiltonian, defined in this way, form a semigroup (without existence of the inverse operation), the renormalization group (RG). The change of the Hamiltonian by the successive cutoff reduction is called renormalization group flow.

We can now perform the renormalization of the Kondo Hamiltonian (or coupling constant $J$) explicitly in a perturbative way, following Anderson [24]. To that end, it is convenient to introduce the dimensionless, bare coupling $g_0 = N(0)J_0$ and running coupling $g = N(0)J$. We also define the projector $P_{\delta D}$ of the conduction electron energy onto the intervals $[-D, -D+\delta D] \cup [D-\delta D, D]$ by which the conduction band is reduced in one RG step as well as the projector $(1-P_{\delta D})$ onto the remaining conduction energy interval, cf. Fig. 3(b). To impose the invariance of physical quantities under the RG flow, it is sufficient to keep the total conduction-electron–pseudo-fermion vertex $\hat{\gamma}_{cf}$ invariant, since all physical quantities are derived from it within the Kondo model. $\hat{\gamma}_{cf}$ is defined by the following T-matrix equation

$$\hat{\gamma}_{cf} = \hat{\gamma}_{cf}^{(1)} + \hat{\gamma}_{cf}^{(1)}\, G\, \hat{\gamma}_{cf}. \tag{25}$$

Here, the bare vertex $\hat{\gamma}_{cf}^{(1)}$ is defined as in Eq. (14), $G$ denotes schematically the product of $G_c$ and $G_f$ propagators connecting two bare vertices $\hat{\gamma}_{cf}^{(1)}$ in the direct and exchange diagrams (cf. Fig. 2), and integration over the conduction electron energy in $G$ is implied. Eq. (25) can be rewritten as

$$\begin{aligned}
\hat{\gamma}_{cf} &= \hat{\gamma}_{cf}^{(1)} + \hat{\gamma}_{cf}^{(1)}\,[P_{\delta D}G]\,\hat{\gamma}_{cf} + \hat{\gamma}_{cf}^{(1)}\,[(1-P_{\delta D})G]\,\hat{\gamma}_{cf} \qquad (26)\\
&= \hat{\gamma}_{cf}^{(1)} + \hat{\gamma}_{cf}^{(1)}\,[P_{\delta D}G]\,\left\{\hat{\gamma}_{cf}^{(1)} + \hat{\gamma}_{cf}^{(1)}\,[(P_{\delta D}+(1-P_{\delta D}))\,G]\,\hat{\gamma}_{cf}\right\} + \hat{\gamma}_{cf}^{(1)}\,[(1-P_{\delta D})G]\,\hat{\gamma}_{cf}\\
&= \hat{\gamma}_{cf}^{(1)\prime} + \hat{\gamma}_{cf}^{(1)\prime}\,[(1-P_{\delta D})G]\,\hat{\gamma}_{cf} \quad + \quad \mathcal{O}(P_{\delta D}^2),
\end{aligned}$$

with

$$\hat{\gamma}_{cf}^{(1)\prime} = \hat{\gamma}_{cf}^{(1)} + \hat{\gamma}_{cf}^{(1)}\,[P_{\delta D}G]\,\hat{\gamma}_{cf}^{(1)} =: \hat{\gamma}_{cf}^{(1)} + \delta\hat{\gamma}_{cf}^{(1)}. \tag{27}$$

In the first line of Eq. (26), the integral over the intermediate conduction electron energy has been split into the infinitesimal high-energy part $P_{\delta D}$ and the remaining part $(1-P_{\delta D})$. In the second line, the high-energy part of the equation has been iterated once, and in the third line, only terms up to linear order in $P_{\delta D}$ have been retained, and all terms have been appropriately rearranged. As seen from the third line, the total vertex $\hat{\gamma}_{cf}$ obeys again a T-matrix equation, however with a reduced conduction bandwidth, $(1-P_{\delta D})$. Moreover, $\hat{\gamma}_{cf}$ remains invariant by this procedure, exactly if the bare vertex is changed to $\hat{\gamma}^{(1)}_{cf}$ as defined in Eq. (27). This is the vertex renormalization we are seeking. Note that this expression is a perturbative, because in Eq. (26) we have iterated the T-matrix equation only once (1-loop approximation). Higher-order iterations, leading to higher-order renormalizations in $\hat{\gamma}^{(1)}_{cf}$ are possible. Note that the vertex renormalization $\delta\hat{\gamma}^{(1)}_{cf}$ in Eq. (27) corresponds just to the 2nd-order perturbation theory expression calculated in Eq. (21), see also Fig. 2. Thus, one can read off from these equations the renormalization of the dimensionless coupling constant $g$ under cutoff reduction $-\delta D$ as

$$dg = -\frac{d}{dD}\left[g^2\int_{-D}^{D} d\varepsilon\,\frac{1-2f(\varepsilon)}{\varepsilon}\right]\delta D = -\frac{2g^2}{D}\,\delta D. \tag{28}$$

Usually one takes the logarithmic derivative which ensures that the differential range $-\delta D$ by which the cutoff is reduced is proportional to the cutoff itself: $\delta D = Dd(\ln D)$. Thus

$$\frac{dg}{d\ln D} = -2g^2. \tag{29}$$

This is the differential renormalization group equation (of 1-loop order). The function on the right-hand side, $\beta(g) = -2g^2$, which controls the running coupling constant renormalization, is called the $\beta$-function of the RG. The RG equation can be integrated in a straightforward way with the initial condition $g(D_0) = g_0$ to give

$$g(D) = \frac{g_0}{1-2g_0\ln(D/D_0)}\,. \tag{30}$$

It is seen that this solution becomes again divergent for antiferromagnetic $g_0 > 0$ when the running cutoff reaches the Kondo scale, $D \to T_K = D_0\exp\left[-1/(2g_0)\right]$, a consequence of the perturbative RG treatment above. However, this divergence allows the conclusion that the ground state of the single-impurity Kondo model is a spin-singlet state between the impurity spin and the spin cloud of the surrounding conduction electron spins as outlined in the introduction. Moreover, it allows for a more general definition of the Kondo spin screening scale $T_K$, namely the value of the running cutoff $D$ where the coupling constant diverges and the singlet starts to be formed. This will be used for the analysis of the Kondo-RKKY interplay in section 4.

# 3 RKKY interaction in paramagnetic and half-metals

In this section we derive the expressions for the RKKY interaction. To be general, we will allow for an arbitrary spin polarization of the conduction band and then specialize for the paramagnetic case (vanishing magnetization) and the half-metallic case (complete magnetization). Thus,

we consider now the Kondo lattice Hamiltonian of localized spins $\hat{\mathbf{S}}_i$ at the lattice positions $\mathbf{r}_i$

$$H = \sum_{\mathbf{k},\sigma} \varepsilon_{\mathbf{k}}\, c^\dagger_{\mathbf{k}\sigma} c_{\mathbf{k}\sigma} + J_0 \sum_i \hat{\mathbf{S}}_i \cdot \hat{\mathbf{s}}_i \,. \tag{31}$$

Usually, the static limit is considered in order to derive a Hamiltonian coupling operator. We will later consider the question of dynamical correlations as well, as it arises in the interplay with the Kondo effect. The interaction Hamiltonian for the conduction electrons and the localized $f$-spin $\mathbf{S}_j$ at a site $j \neq i$,

$$H^{(cf)}_j = J_0 \hat{\mathbf{S}}_j \cdot \hat{\mathbf{s}}_j \,, \tag{32}$$

acts as a perturbation for the localized $f$-spin at a site $i$ (and vice versa). Performing standard thermal perturbation theory by expanding the time evolution operator in the interaction picture, $\hat{T}\exp[-\int_0^\beta d\tau H^{cf}_j(\tau)]$ up to linear order in $J_0$, one obtains for the interaction operator of the $f$-spin at site $i$ up to $\mathcal{O}(J_0^2)$

$$H^{(2)}_{ij} = J_0\, \hat{\mathbf{S}}_i \cdot \hat{\mathbf{s}}_i \;-\; J_0^2\, \langle (\hat{\mathbf{S}}_i \cdot \hat{\mathbf{s}}_i)(\hat{\mathbf{S}}_j \cdot \hat{\mathbf{s}}_j) \rangle_c \Big|_{\omega=0} \,. \tag{33}$$

Here, $\langle (\dots) \rangle_c := \mathrm{tr}_c\{\mathrm{e}^{-\beta H}(\dots)\}/Z_G$, denotes the thermal trace over the conduction electron Hilbert space, and the static limit, $\omega = 0$, has been taken. Using Wick's theorem with respect to the conduction electron operators, the second term in Eq. (33) can be written as

$$H^{RKKY}_{ij} = -\frac{J_0^2}{4} \sum_{\alpha,\beta=x,y,z} \sum_{\sigma\sigma'} \hat{S}^\alpha_i\, \sigma^\alpha_{\sigma\sigma'} \sigma^\beta_{\sigma'\sigma}\, \hat{S}^\beta_j \Pi^{\sigma\sigma'}_{ij}(0), \tag{34}$$

where $\hat{S}^\alpha_i$, $\alpha = x,\, y,\, z$, are the components of the impurity spin, $\sigma^\alpha$ the Pauli matrices, and $\Pi^{\sigma\sigma'}_{ij}$ the conduction electron density propagator between the sites $i$ and $j$ as depicted diagrammatically in Fig. 4(a). It has the general form,

$$\Pi^{\sigma\sigma'}_{ij}(i\omega) = -\frac{1}{\beta} \sum_{\varepsilon_n} G_{ji\,\sigma}(i\varepsilon_n + i\omega) G_{ij\,\sigma'}(i\varepsilon_n) \,. \tag{35}$$

In the static limit it reads

$$\Pi^{\sigma\sigma'}_{ij}(0) = -\int d\varepsilon\; f(\varepsilon)\, [A_{ij\,\sigma}(\varepsilon) \mathrm{Re} G_{ij\,\sigma'}(\varepsilon) + A_{ij\,\sigma'}(\varepsilon) \mathrm{Re} G_{ij\,\sigma}(\varepsilon)] \,,$$

where $A_{ij\,\sigma}(\varepsilon) = -\mathrm{Im} G_{ij\,\sigma}(\varepsilon + i0)/\pi$. Performing the spin contractions in Eq. (34) and defining the longitudinal and the transverse polarization functions, respectively, as

$$\Pi^{||}_{ij}(0) \;=\; \frac{1}{2} \sum_\sigma \Pi^{\sigma\sigma}_{ij}(0) \;= -\sum_\sigma \int d\varepsilon\, f(\varepsilon)\, A_{ij\,\sigma}(\varepsilon)\, \mathrm{Re}\, G_{ij\,\sigma}(\varepsilon) \tag{36}$$

$$\Pi^{\perp}_{ij}(0) \;=\; \frac{1}{2} \sum_\sigma \Pi^{\sigma\,-\sigma}_{ij}(0) = -\sum_\sigma \int d\varepsilon\, f(\varepsilon)\, A_{ij\,\sigma}(\varepsilon)\, \mathrm{Re}\, G_{ij\,-\sigma}(\varepsilon) \,, \tag{37}$$

one obtains the RKKY interaction Hamiltonian,

$$H^{RKKY} = \sum_{i\neq j} H^{RKKY}_{ij} = -\sum_{i,j} \left[ K^{||}_{ij}\, \hat{S}^z_i \hat{S}^z_j - K^\perp_{ij} \left( \hat{S}^x_i \hat{S}^x_j + \hat{S}^y_i \hat{S}^y_j \right) \right]$$

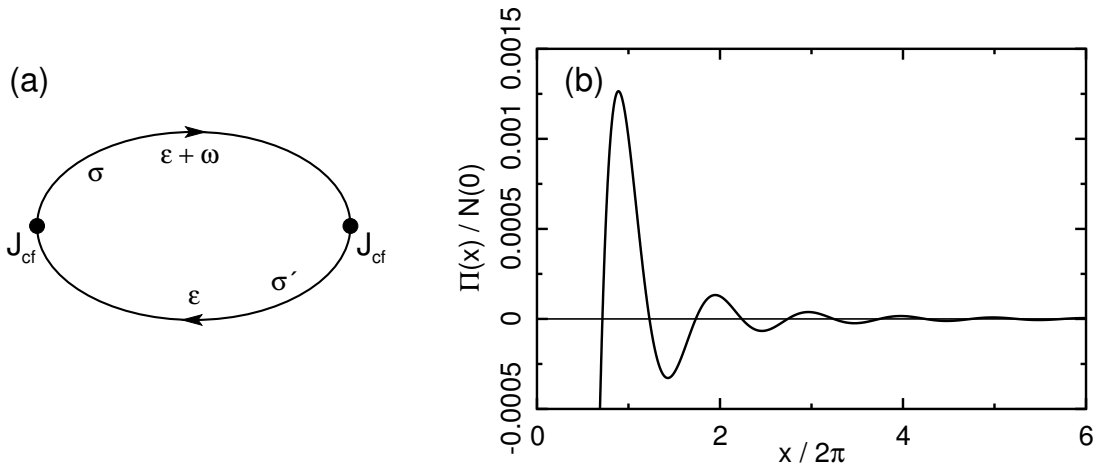


**Fig. 4:** *(a) Diagram for the spin-dependent conduction electron polarization function $\Pi_{ij}^{\sigma\sigma'}(\omega)$, generating the RKKY interaction. The solid lines represent conduction electron propagators. (b) Oscillatory behavior of $\Pi_{ij}^{\sigma\sigma'}(0)$ in a paramagnetic metal with isotropic dispersion as a function of distance $x = 2k_F|\mathbf{r}_i - \mathbf{r}_j|$, Eq. (45)*

where the sums run over all (arbitrarily distant) lattice sites $i,\ j, i \neq j$ of localized spins $\hat{\mathbf{S}}_i$ and $\hat{\mathbf{S}}_j$, and

$$K_{ij}^{||} = \frac{1}{2} J_0^2 \Pi_{ij}^{||}(0) \ , \qquad K_{ij}^{\perp} = \frac{1}{2} J_0^2 \Pi_{ij}^{\perp}(0) \ , \tag{38}$$

are the longitudinal and transverse RKKY couplings, respectively. The spin being a vector operator, the interaction Hamiltonian $H_{ij}^{RKKY}$ has a tensor structure and is, in general, anisotropic for a magnetized conduction band, as seen from Eq. (38).

We now present explicitly the expressions for the special cases of a paramagnet and of a half-metal. For a paramagnetic conduction band we have $G_{ij\,\sigma} = G_{ij,-\sigma}$, independent of spin. Hence, the RKKY coupling is isotropic, and we have the paramagnetic RKKY Hamiltonian,

$$H_{PM}^{RKKY} = -\sum_{(i,j)} K_{ij}^{PM}\, \hat{\mathbf{S}}_i \cdot \hat{\mathbf{S}}_j \ , \tag{39}$$

with

$$K_{ij}^{PM} = -\frac{J_0^2}{2} \sum_{\sigma} \int d\varepsilon\, f(\varepsilon)\, A_{ij\,\sigma}(\varepsilon)\, \mathrm{Re}\, G_{ij\,\sigma}(\varepsilon) \ . \tag{40}$$

For a half-metal, i.e., for a completely spin-magnetized conduction band with majority spin $\sigma = \uparrow$ we have $A_{ij\downarrow}(\varepsilon) = 0$, Thus, the half-metallic RKKY Hamiltonian reads

$$H_{FM}^{RKKY} = -\sum_{(i,j)} \left[ K_{ij}^{FM\,||}\, \hat{S}_i^z \hat{S}_j^z + K_{ij}^{FM\,\perp} \left( \hat{S}_i^x \hat{S}_j^x + \hat{S}_i^y \hat{S}_j^y \right) \right] \ , \tag{41}$$

with

$$K_{ij}^{FM\,||} = -\frac{J_0^2}{2} \int d\varepsilon\, f(\varepsilon)\, A_{ij\uparrow}(\varepsilon)\ \mathrm{Re}\, G_{ij\uparrow}(\varepsilon) \tag{42}$$

$$K_{ij}^{FM\,\perp} = -\frac{J_0^2}{2} \int d\varepsilon\, f(\varepsilon)\, A_{ij\uparrow}(\varepsilon)\ \mathrm{Re}\, G_{ij\downarrow}(\varepsilon) \ . \tag{43}$$

The missing spin summation in Eqs. (42) and (43) as compared to Eq. (40) indicates that in the completely magnetized band only the majority spin species contributes to the coupling. Note, however, that the transverse coupling $K_{ij}^{FM\perp}$ is still non-zero even in the ferromagnetically saturated case because of virtual (off-shell) minority spin contributions represented by the real part $\mathrm{Re}\, G_{ij\downarrow}(\varepsilon)$ in Eq. (43).

The RKKY coupling is long-ranged and has in general complex, oscillatory behavior in space, because it depends on details of the conduction band structure via the position dependent Green functions $G_{ji\,\sigma}(\omega)$ in Eq. (35). For an isotropic system in $d = 3$ dimensions, the retarded/advanced conduction electron Green function $G_{r\sigma}(\varepsilon \pm i0)$ and the paramagnetic polarization $\Pi_r^{\sigma\sigma'}(\omega)$ at temperature $T = 0$ are calculated in position space as,

$$G_{r\sigma}(\varepsilon \pm i0) = -\pi N(\varepsilon)\, \frac{\mathrm{e}^{\pm ik(\varepsilon_F+\varepsilon)r}}{k(\varepsilon_F+\varepsilon)r} \tag{44}$$

$$\begin{aligned} \Pi_r^{\sigma\sigma'}(\omega + i0) = & \left[ N(0)\, \frac{\sin(x) - x\cos(x)}{4x^4} + \mathcal{O}\left( \left( \frac{\omega}{\varepsilon_F} \right)^2 \right) \right] \\ & \pm i \left[ \frac{1}{\pi} N(0)\, \frac{1-\cos(x)}{x^2}\, \frac{\omega}{\varepsilon_F} + \mathcal{O}\left( \left( \frac{\omega}{\varepsilon_F} \right)^3 \right) \right] \end{aligned} \tag{45}$$

Here, $\varepsilon_F$ and $k_F$ are the Fermi energy and Fermi wavenumber, respectively, and $r = |\mathbf{r}_i - \mathbf{r}_j|$, $x = 2k_F r$. For illustration, Fig. 4(b) shows the static polarization $\Pi_r^{\sigma\sigma'}(0)$ as a function of $x$ for the isotropic case.

# 4 Interplay of Kondo screening and RKKY interaction

We now turn to the interplay of the two interactions on a Kondo lattice, Eq. (31). First, it is crucial to remember that the RKKY interaction between different $f$-spins is not a direct spin exchange interaction, but mediated by the conduction band [3–5] and generated in second order by the same spin coupling $J_0$ that is also responsible for the local Kondo spin screening, as shown in the previous section. The essential difference can be seen from the example of a two-impurity Kondo system, $\mathbf{S}_1$, $\mathbf{S}_2$: With a direct impurity-impurity coupling, $K\,\mathbf{S}_1 \cdot \mathbf{S}_2$, this model can exhibit a dimer singlet phase where the dimer is decoupled from the conduction electrons. The dimer singlet and the local Kondo singlet phase are then separated by a quantum critical point (QCP), controlled by $K$ [25, 26]. By contrast, when the inter-impurity coupling is created by the RKKY interaction only, i.e. generated by $J_0$, a decoupled dimer singlet phase is not possible. Instead, the impurity spins must remain coupled to the conduction sea. We show below that the Kondo singlet formation at $T = 0$ breaks down at a critical strength of the RKKY coupling even if magnetic ordering is suppressed, i.e. without a 2nd-order quantum phase transition and without critical fluctuations. If magnetic ordering occurs, critical ordering fluctuations will be present in addition to, but independently of the RKKY-induced Kondo breakdown.

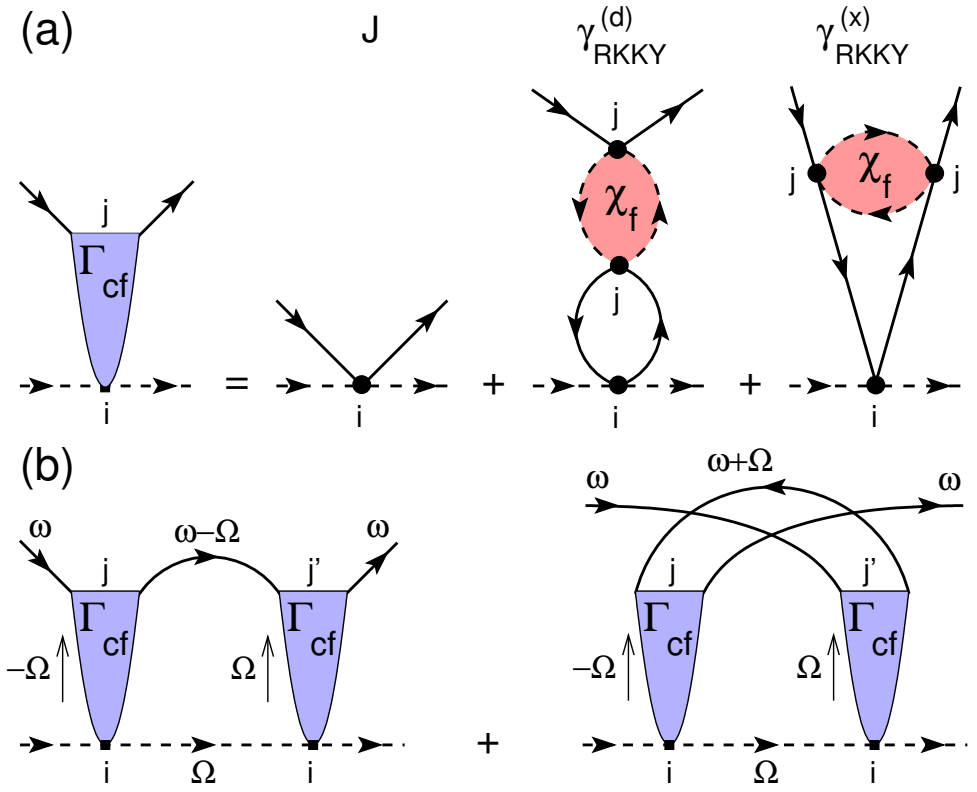


**Fig. 5:** *(a) $f$-spin–$c$-electron vertex $\hat{\Gamma}_{cf}$, composed of the onsite vertex $J$ at site $i$ and the RKKY-induced contributions from surrounding sites $j \neq i$ to leading order in the RKKY coupling, $\gamma^{(d)}_{RKKY}$ (direct term) and $\gamma^{(x)}_{RKKY}$ (exchange term). (b) 1-loop diagrams for the perturbative RG. Solid lines: electron Green functions $G_c$, dashed lines: pseudo-fermion propagators $G_f$ of the local $f$-spins. The red bubbles represent the full $f$-spin susceptibility at sites $j$.*

## 4.1 The concept of a selfconsistent renormalization group

The problem of local Kondo screening or breakdown on a Kondo lattice amounts to calculating the vertex for scattering of $c$-electrons from a local $f$-spin and analyzing its divergence (Kondo screening of the $f$-spin, cf. section 2.3) or non-divergence (Kondo breakdown) under RG. In the case of multiple Kondo sites or a Kondo lattice, this vertex $\hat{\Gamma}_{cf}$ acquires nonlocal contributions in addition to the local coupling $J_0$, because a $c$-electron can scatter from a distant Kondo site $j \neq i$, and the spin flip at that site is transferred to the $f$-spin at site $i$ via the RKKY interaction. On the other hand, the RKKY vertex $\hat{\Gamma}_{ff}$ coupling two $f$-spins has no logarithmic RG flow, since the recoil (momentum integration) of the itinerant conduction electrons prevents an infrared divergence of the RKKY interaction. Thus, $\hat{\Gamma}_{ff}$ remains in the weak coupling regime, and RKKY-induced magnetic ordering must be a secondary effect, not controlled by the RG divergence of a coupling constant.

The diagrams contributing to $\hat{\Gamma}_{cf}$ to leading order in the RKKY coupling are shown in Fig. 5(a). As seen from the figure, a nonlocal scattering process necessarily involves the exact, local dynamical $f$-spin susceptibility $\chi_f(i\Omega_n)$ on site $j$. The resulting $c$–$f$ vertex $\hat{\Gamma}_{cf}$ has the structure of a nonlocal Heisenberg coupling in spin space, see Appendix A.1. The exchange diagram,

$\gamma^{(x)}_{RKKY}$ in Fig. 5(a), contributes only a sub-leading logarithmic term as compared to the direct term $\gamma^{(d)}_{RKKY}$, see Appendix A.2. In particular, it does not alter the universal $T_K(y)$ suppression derived below. It can, therefore, be neglected. To leading (linear) order in the RKKY coupling, $\hat{\Gamma}_{cf}$ thus reads (in Matsubara representation)

$$\begin{aligned} \hat{\Gamma}_{cf} &= \left[J\delta_{i,j} + \gamma^{(d)}_{RKKY}(\mathbf{r}_{ij}, i\Omega_n)\right] \mathbf{S}_i \cdot \mathbf{s}_j \\ &= \left[J\delta_{ij} + 2J J_0^2\,(1-\delta_{ij})\; \Pi(\mathbf{r}_{ij}, i\Omega_n)\, \tilde{\chi}_f(i\Omega_n)\right] \mathbf{S}_i \cdot \mathbf{s}_j\,, \end{aligned} \tag{46}$$

where $\mathbf{r}_{ij} = \mathbf{x}_i - \mathbf{x}_j$ the distance vector between the sites $i$ and $j$, and $\Omega$ is the energy transferred in the scattering process. $\Pi(\mathbf{r}_{ij}, i\Omega_n)$ is the $c$-electron density correlation function between sites $i$ and $j$ [bubble of solid lines in Fig. 5(a)] and $\tilde{\chi}_f(i\Omega_n) := \chi_f(i\Omega_n)/(g_L\mu_B)^2$, with $g_L$ the Landé factor and $\mu_B$ the Bohr magneton. Note that Eq. (46) contains the running coupling $J$ at site $i$ which will be renormalized under RG, while at the site $j$, where the $c$-electron scatters, the bare coupling $J_0$ appears, since all vertex renormalizations on that site are already included in the exact susceptibility $\chi_f$. Higher order terms, as for instance generated by the RG [see below, Fig. 5(b)], lead to nonlocality of the incoming and outgoing coordinates of the scattering $c$-electrons, $\mathbf{x}_j$, $\mathbf{x}_{j'}$, but the $f$-spin coordinate $\mathbf{x}_i$ remains strictly local, since the pseudo-fermion propagator $G_f(i\nu_n) = 1/i\nu_n$ is local [20]. For this reason, speaking of Kondo singlet formation on a single Kondo site is well defined even on a Kondo lattice, and so is the local susceptibility $\chi_f$ of a single $f$-spin. The corresponding Kondo scale $T_K$ on a site $j$ is observable, e.g., as the Kondo resonance width measured by STM spectroscopy on one Kondo ion of the Kondo lattice. The temperature dependence of the single-site $f$-spin susceptibility is known from the Bethe ansatz solution [22] in terms of the Kondo scale $T_K$. It has a $T = 0$ value $\chi_f(0) \propto 1/T_K$ and crosses over to the $1/T$ behavior of a free spin for $T > T_K$. These features can be modeled in the retarded/advanced, local, dynamical $f$-spin susceptibility $\chi_f(\Omega \pm i0)$ as

$$\chi_f(\Omega \pm i0) = \frac{(g_L\mu_B)^2 W}{\pi T_K \sqrt{1 + (\Omega/T_K)^2}} \left(1 \pm \frac{2i}{\pi} \mathrm{arsinh} \frac{\Omega}{T_K}\right) \tag{47}$$

where $W$ is the Wilson ratio, and the imaginary part is implied by the Kramers-Kronig relation. Deriving the one-loop RG equation for a multi-impurity or lattice Kondo system proceeds as in section 2.3, however for the $c$–$f$ vertex $\hat{\Gamma}_{cf}$, including RKKY-induced nonlocal contributions. The one-loop spin vertex function is shown diagrammatically in Fig. 5(b). Using Eq. (46), the sum of these two diagrams is up to linear order in the RKKY coupling,

$$\begin{aligned} Y(\mathbf{r}_{ij}, i\omega_n) = -J\,T \sum_{i\Omega_m} &\left[J\delta_{ij} + \gamma^{(d)}_{RKKY}(\mathbf{r}_{ij}, i\Omega_m) + \gamma^{(d)}_{RKKY}(\mathbf{r}_{ij}, -i\Omega_m)\right] \\ &\times \left[G_c(\mathbf{r}_{ij}, i\omega_n - i\Omega_m) - G_c(\mathbf{r}_{ij}, i\omega_n + i\Omega_m)\right]\, G_f(i\Omega_m). \end{aligned} \tag{48}$$

Here, $\omega$ is the energy of incoming conduction electrons and $G_c(\mathbf{r}_{ij}, i\omega_n + i\Omega_m)$ the single-particle $c$-electron propagator from the incoming to the outgoing site.

For the low-energy physics, the vertex renormalization for $c$-electrons at the Fermi surface is required. This means setting the energy $i\omega \to \omega = 0 + i0$ and Fourier transforming the total

vertex $Y(\mathbf{r}_{ij}, i\omega)$ with respect to the incoming and outgoing $c$-electron coordinates, $\mathbf{x}_j$, $\mathbf{x}_i$, and taking its Fourier component for momenta at the Fermi surface, $\mathbf{k}_F$. Note that at the Fermi energy $Y(\mathbf{k}_F, 0)$ is real, even though the RKKY-induced, dynamical vertex $\gamma^{(d)}_{RKKY}(\pm i\Omega_m)$ appearing in Eq. (48) is complex-valued. This ensures the total vertex operator of the renormalized Hamiltonian to be Hermitian. By analytic continuation, the Matsubara summation in Eq. (48) becomes an integration over the intermediate $c$-electron energy from the lower and upper band cutoff $\mp D$ to the Fermi energy ($\Omega = 0$). The coupling constant renormalization is then obtained by requiring that $Y(\mathbf{k}_F, 0)$ is invariant under an infinitesimal reduction of the running band cutoff $D$ (cf. section 2.3). Note that the band cutoff appears in both, the intermediate electron propagator $G_c$ and in $\Pi$. However, differentiation of the latter does not contribute to the logarithmic RG flow. This leads to the 1-loop lattice RG equation for the local coupling [27]

$$\frac{\mathrm{d}g}{\mathrm{d}\ln D} = -2g^2 \left(1 - y\, g_0^2\, \frac{D_0}{T_K}\, \frac{1}{\sqrt{1+(D/T_K)^2}}\right), \tag{49}$$

with the bare band cutoff $D_0$. The first term in Eq. (49) is the onsite contribution to the $\beta$-function, while the second term represents the RKKY contribution. It is seen that $\chi_f$, as in Eq. (47), induces a soft cutoff on the scale $T_K$ and the characteristic $1/T_K$ dependence to the RG flow of this contribution, where $T_K$ is the Kondo scale on the *surrounding* Kondo sites. The dimensionless coefficient

$$y = -\frac{8W}{\pi^2}\mathrm{Im}\sum_{j\neq i}\frac{\mathrm{e}^{-i\mathbf{k}_F\mathbf{r}_{ij}}}{N(0)^2}G^R_c(\mathbf{r}_{ij}, \Omega=0)\,\Pi(\mathbf{r}_{ij}, \Omega=0) \tag{50}$$

arises from the Fourier transform $Y(\mathbf{k}_F, 0)$ and parameterizes the RKKY coupling strength. The summation in Eq. (50) runs over all positions $j \neq i$ of Kondo sites in the system. It is important to note that $y$ is generically positive, even though the RKKY correlations $\Pi(\mathbf{r}_{ij}, 0)$ may be ferro- or antiferromagnetic. For instance, for an isotropic and dense system with lattice constant $a$ ($k_F a \ll 1$), the summation in Eq. (50) can be approximated by an integral, and with the substitution $x = 2k_F|\mathbf{r}_{ij}|$, $y$ can be expressed as

$$y \approx \frac{2W}{(k_F a)^3}\int_{k_F a}^{\infty} dx\,(1-\cos x)\,\frac{x\cos x - \sin x}{x^4} > 0\,. \tag{51}$$

As a consequence, the RKKY correlations reduce the $g$-renormalization in Eq. (49), irrespective of the sign of $\Pi(\mathbf{r}_{ij}, 0)$, as one would physically expect.

The Kondo scale for singlet formation on site $i$ is defined as the running cutoff value where the $c$–$f$ coupling $g$ diverges. An important feature of the lattice RG equation (49) is that the Kondo screening scale on surrounding sites $j \neq i$ appears as a parameter in the $\beta$-function for the renormalization on site $i$. By equivalence of all Kondo sites, the Kondo scales $T_K$ on all sites $i$ and $j$ must be equal. This leads to the fact that the divergence scale $T_K$ of the lattice RG equation must be determined self-consistently and will imply an implicit equation for the local screening scale $T_K = T_K(y)$ on a Kondo lattice, which will depend on the RKKY parameter $y$. The equivalence of the $c$–$f$ vertices on all Kondo sites is reminiscent of a dynamical mean-field theory treatment, however, it goes beyond the latter in taking the long-range RKKY contributions into account.

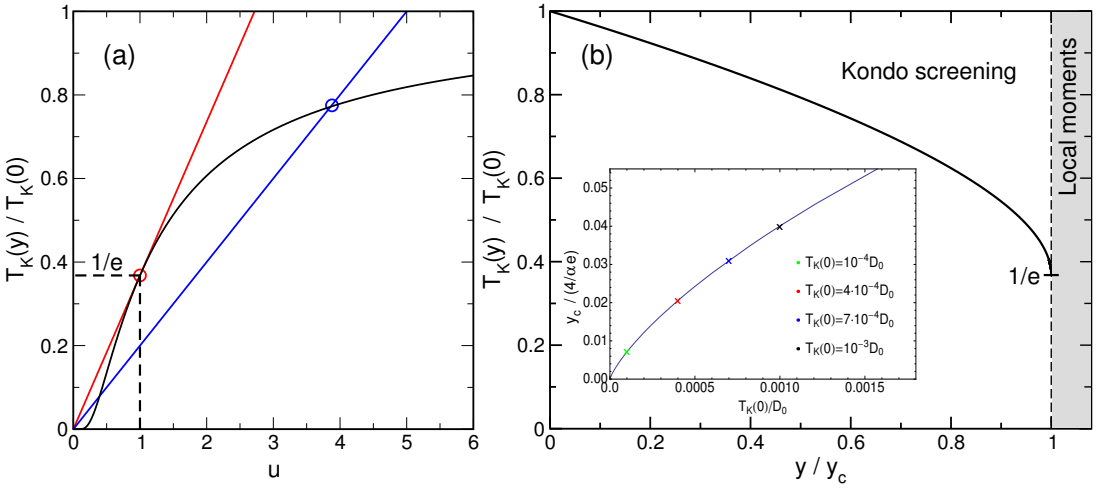


**Fig. 6:** *(a) Graphical solution of Eq. (55): black, solid curve: right-hand side of Eq. (55), blue line: left-hand side for $y < y_c$, red line: left-hand side for $y = y_c$ (where red line and black curve touch). It proves that there is a critical coupling $y_c$ beyond which Eq. (55) has no solution, and $T_K(y_c)/T_K(0) = 1/e$. (b) Universal dependence of $T_K(y)/T_K(0)$ on the normalized RKKY parameter $y/y_c$, solution of Eq. (55). The inset shows the critical RKKY parameter $y_c$ for various single-ion Kondo temperatures $T_K(0)$, Eq. (57).*

## 4.2 Integration of the RG equation

The RG equation Eq. (49) is readily integrated by separation of variables,

$$-\int_{g_0}^{g}\frac{dg}{g^2} \;=\; 2\int_{\ln D_0}^{\ln D} d\ln D' \;-\; 2yg_0^2\frac{D_0}{T_K}\int_{D_0/T_K}^{D/T_K}\frac{dx}{x}\frac{1}{\sqrt{1+x^2}}\,, \tag{52}$$

or

$$\frac{1}{g}-\frac{1}{g_0} \;=\; 2\ln\left(\frac{D}{D_0}\right) \;-\; yg_0^2\frac{D_0}{T_K}\ln\left(\frac{\sqrt{1+(D/T_K)^2}-1}{\sqrt{1+(D/T_K)^2}+1}\right), \tag{53}$$

where we have used $D_0/T_K \gg 1$ in the last expression. The Kondo scale is defined as the value of the running cutoff $D$ where $g$ diverges, i.e., $g \to \infty$ when $D \to T_K$. This yields the defining equation for the Kondo scale $T_K \equiv T_K(y)$,

$$-\frac{1}{g_0} \;=\; 2\ln\left(\frac{T_K(y)}{D_0}\right) \;-\; yg_0^2\frac{D_0}{T_K(y)}\ln\left(\frac{\sqrt{2}-1}{\sqrt{2}+1}\right).$$

Using the definition of the single-impurity Kondo temperature, $-1/g_0 = 2\ln\left(T_K(0)/D_0\right)$, the defining, implicit equation for $T_K(y)$ can finally be written as

$$\frac{T_K(y)}{T_K(0)} = \exp\left(-y\,\alpha\,g_0^2\,\frac{D_0}{T_K(y)}\right)\,, \tag{54}$$

with $\alpha = \ln(\sqrt{2}+1)$.

## 4.3 Universal suppression of the Kondo scale

By the rescaling, $u = T_K(y)/(y\alpha g_0^2 D_0)$, $y_c = T_K(0)/(\alpha \mathrm{e} g_0^2 D_0)$, Eq. (54) takes the universal form (e is Euler's constant),

$$\frac{y}{\mathrm{e}y_c}\,u = \mathrm{e}^{-1/u}\,. \tag{55}$$

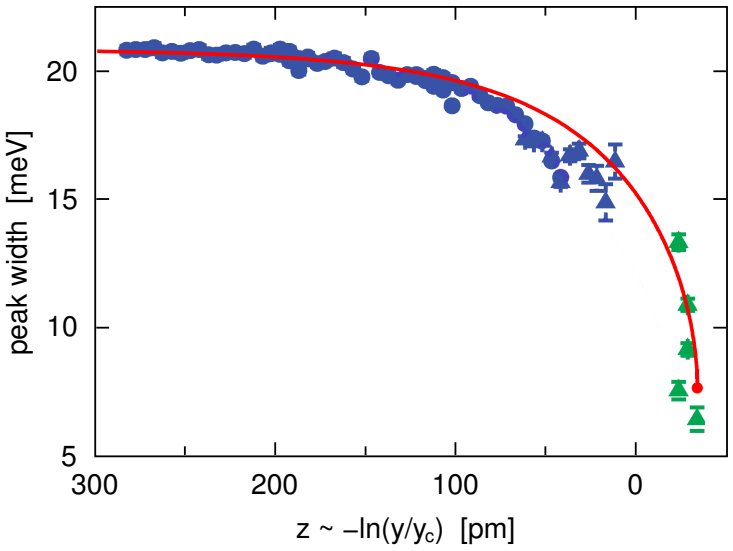


**Fig. 7:** *Comparison of the theory (red curve), Eq. (55), with STM spectroscopy experiments on a tunable two-impurity Kondo system (data points, Ref. [29]). The data points represent the Kondo scale $T_K$ as extracted from the STM spectra by fitting a split Fano line shape of width $T_K$ to the experimental spectra, see [29] for experimental details.*

Its solution can be expressed in terms of the Lambert $W$ function [28] as $u(y) = -1/W(-y/\mathrm{e}y_c)$. Fig. 6(a) visualizes solving Eq. (55) graphically. It shows that Eq. (55) has solutions only for $y \leq y_c$. This means that $y_c$ marks a Kondo breakdown point beyond which the RG does not scale to strong coupling, i.e., a Kondo singlet is not formed for $y > y_c$ even at the lowest energies. Using the above definitions, the RKKY-induced suppression of the Kondo lattice temperature reads, $T_K(y)/T_K(0) = u(y)y/(\mathrm{e}y_c) = -y/[\mathrm{e}y_c W(-y/\mathrm{e}y_c)]$. It is shown in Fig. 6(b). In particular, at the breakdown point it vanishes *discontinuously* and takes the finite, universal value (see Fig. 6(a)),

$$\frac{T_K(y_c)}{T_K(0)} = \frac{1}{\mathrm{e}} \approx 0.368\,. \tag{56}$$

We emphasize that the RKKY parameter $y$ depends on details of the conduction band structure and of the spatial arrangement of Kondo sites. Sub-leading contributions to $\Gamma_{cf}$ may modify the form of the cutoff function in the RG Eq. (49) and thus the nonuniversal parameter $\alpha$. However, all this does not affect the universal dependence $T_K(y)$ on $y$ given by Eq. (55).

The critical RKKY parameter, as defined before Eq. (55), can be expressed solely in terms of the single-ion Kondo scale,

$$y_c = \frac{4}{\alpha \mathrm{e}} \tau_K (\ln \tau_K)^2\,, \tag{57}$$

with $\tau_K = T_K(0)/D_0$. Note that [via $T_K(0) = D_0 \exp(-1/2g_0)$ and $N(0) = 1/(2D_0)$] this is equivalent to Doniach's breakdown criterion [7], $N(0) y_c J_0^2 = T_K(0)$, up to a factor of $\mathcal{O}(1)$. However, the present theory goes beyond the Doniach scenario in that it predicts the behavior of $T_K(y)$.

The present theory applies directly to two-impurity Kondo systems, where magnetic ordering does not play a role, and can be compared to corresponding STM experiments [29, 30]. In Ref. [29], the Kondo scale has been extracted as the line width of the (hybridization-split)

Kondo-Fano resonance. In this experimental setup, the RKKY parameter $y$ is proportional to the overlap of tip and surface $c$-electron wave functions and, thus, depends exponentially on the tip-surface separation $z$, $y = y_c \exp(-(z - z_0)/\xi)$. Identifying the experimentally observed breakdown point, $z = z_0$, with the Kondo breakdown point, the only adjustable parameters are a scale factor $\xi$ of the $z$ coordinate and $T_K(0)$, the resonance width at large separation, $z = 300$ pm. The agreement between theory and experiment is striking, as shown in Fig. 7. In particular, at the breakdown point $T_K(y_c)/T_K(0)$ coincides accurately with the prediction, Eq. (56), without any adjustable parameters.

# 5 Conclusion

We have derived a perturbative renormalization group theory for the interference of Kondo singlet formation and RKKY interaction in Kondo lattice and multi-impurity systems, assuming that magnetic ordering is suppressed, e.g. by frustration. Eqs. (54) or (55) represent a mathematical definition of the energy scale for Kondo singlet formation in a Kondo lattice, i.e., of the Kondo lattice temperature, $T_K(y)$. The theory predicts a universal suppression of $T_K(y)$ and a breakdown of complete Kondo screening at a critical RKKY parameter, $y = y_c$. At the breakdown point, the Kondo scale takes a *finite*, universal value, $T_K(y_c)/T_K(0) = 1/\mathrm{e} \approx 0.368$, and vanishes *discontinuously* for $y > y_c$. In the Anderson lattice, by contrast to the Kondo lattice, the locality of the $f$-spin does no longer strictly hold, but our approach should still be valid in this case. The parameter-free, quantitative agreement of this behavior with different spectroscopic experiments [29, 30] strongly supports that the present theory captures the essential physics of the Kondo-RKKY interplay.

The results may have profound relevance for heavy-fermion magnetic QPTs. In an unfrustrated lattice, the partially screened local moments existing for $y > y_c$ must undergo a second-order magnetic ordering transition at sufficiently low temperature. This means that the bare $c$-electron correlation or polarization function $\Pi$ must be replaced by the full $c$-correlation function $\chi_c$ and will imply a power-law divergence of the latter in Eq. (46). We have checked the effect of such a magnetic instability, induced either by the ordering of remanent local moments or by a $c$-electron SDW instability: The breakdown ratio $T_K(y_c)/T_K(0)$ will be altered, but must remain nonzero. The reason is that the inflection point of the exponential on the right-hand side of Eq. (55) (see Fig. 6) is not removed by such a divergence and, therefore, the solution ceases to exist at a finite value of $T_K(y_c)$. This points to an important conjecture about a possible, new quantum critical scenario with Kondo destruction: The Kondo spectral weight may vanish continuously at the QCP, while the Kondo energy scale $T_K(y)$ (resonance width) remains finite. Such a scenario may reconcile apparently contradictory experimental results in that it may fulfill dynamical scaling, even though $T_K(y_c)$ is finite at the QCP.

# Appendix

# A $f$-spin – conduction-electron vertex $\hat{\Gamma}_{cf}$

Here we present some details on the calculation of the elementary $c$-electron–$f$-spin vertex $\hat{\Gamma}_{cf}$ It is defined via the Kondo lattice Hamiltonian,

$$H = \sum_{\mathbf{k},\sigma} \varepsilon_{\mathbf{k}}\, c^{\dagger}_{\mathbf{k}\sigma} c_{\mathbf{k}\sigma} + J_0 \sum_i \hat{\mathbf{S}}_i \cdot \hat{\mathbf{s}}_i \;, \tag{58}$$

The direct ($d$) and exchange ($x$) parts of the RKKY-induced vertex can be written as the product of a distance and energy dependent function $\Lambda^{(d/x)}_{RKKY}$ and an operator in spin space, $\hat{\Gamma}^{(d/x)}$,

$$\hat{\gamma}^{(d/x)}_{RKKY} = \Lambda^{(d/x)}_{RKKY}(\mathbf{r}_{ij}, i\Omega)\, \hat{\Gamma}^{(d/x)} \tag{59}$$

## A.1 Spin structure

Denoting the vector of Pauli matrices acting in $c$-electron spin space by $\boldsymbol{\sigma} = (\sigma^x, \sigma^y, \sigma^z)^T$ and the vector of Pauli matrices in $f$-spin space by $\mathbf{s} = (s^x, s^y, s^z)^T$, the RRKY-induced vertex contributions read in spin space,

$$\hat{\Gamma}^{(d)}_{\alpha\beta,\kappa\lambda} = \sum_{a,b,c=x,y,z} \sum_{\gamma,\delta,\mu,\nu=1}^{2} \left(\sigma^a_{\delta\gamma} s^a_{\kappa\lambda}\right) \left(\sigma^b_{\gamma\delta} s^b_{\nu\mu}\right) \left(\sigma^c_{\alpha\beta} s^c_{\mu\nu}\right) \tag{60}$$

$$\hat{\Gamma}^{(x)}_{\alpha\beta,\kappa\lambda} = \sum_{a,b,c=x,y,z} \sum_{\gamma,\delta,\mu,\nu=1}^{2} \left(\sigma^a_{\delta\gamma} s^a_{\kappa\lambda}\right) \left(\sigma^b_{\alpha\delta} s^b_{\nu\mu}\right) \left(\sigma^c_{\gamma\beta} s^c_{\mu\nu}\right) \tag{61}$$

with $c$-electron spin indices $\alpha$, $\beta$, $\gamma$, $\delta$, and $f$-spin indices $\kappa$, $\lambda$, $\mu$, $\nu$, as shown in Fig. 8(a). The spin summations can be performed using the spin algebra ($a, b = x, y, z$),

$$\sum_{\gamma=1}^{2} \sigma^a_{\alpha\gamma} \sigma^b_{\gamma\beta} = \sum_{c=x,y,z} i\varepsilon^{abc} \sigma^c_{\alpha\beta} + \delta^{ab} \mathbb{1}_{\alpha\beta} \;, \tag{62}$$

where $\mathbb{1}$ is the unit operator in spin space, $\varepsilon^{abc}$ the totally antisymmetric tensor and $\delta^{ab}$ the Kronecker-$\delta$. This results in a nonlocal Heisenberg coupling between sites $i$ and $j$,

$$\hat{\Gamma}^{(d)}_{\alpha\beta,\kappa\lambda} = 4 \sum_{a=x,y,z} \left(\sigma^a_{\alpha\beta} s^a_{\kappa\lambda}\right) \tag{63}$$

$$\hat{\Gamma}^{(x)}_{\alpha\beta,\kappa\lambda} = -2 \sum_{a=x,y,z} \left(\sigma^a_{\alpha\beta} s^a_{\kappa\lambda}\right) \;. \tag{64}$$

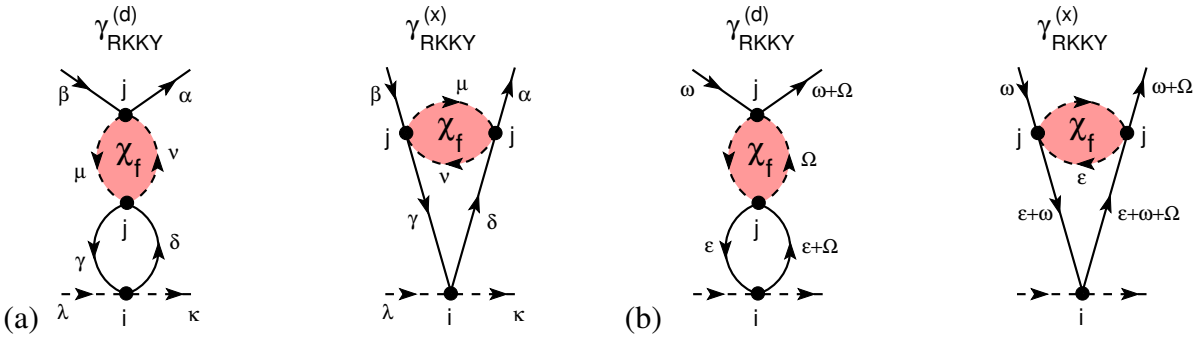


**Fig. 8:** *Direct ($d$) and exchange ($x$) diagrams of the RKKY-induced contributions to the $c$–$f$ vertex: (a) spin labelling, (b) energy labelling.*

## A.2 Energy dependence

With the energy variables as defined in Fig. 8(b), the energy dependent functions in Eq. (59) read in Matsubara representation

$$\Lambda^{(d)}_{RKKY}(\mathbf{r}_{ij}, i\Omega_m) = JJ_0^2 \Pi(\mathbf{r}_{ij}, i\Omega_m)\tilde{\chi}_f(i\Omega_m)$$
$$\Lambda^{(x)}_{RKKY}(\mathbf{r}_{ij}, i\omega_n, i\Omega_m) = -JJ_0^2 T \sum_{i\varepsilon_m} G_c(\mathbf{r}_{ij}, i\omega_n + i\varepsilon_m) G_c(\mathbf{r}_{ij}, i\omega_n + i\Omega_m + i\varepsilon_m)\tilde{\chi}_f(i\varepsilon_m)$$

where

$$\Pi(\mathbf{r}_{ij}, i\Omega_m) \;=\; -T\sum_{\varepsilon_n} G_c(\mathbf{r}_{ij}, i\varepsilon_n) G_c(\mathbf{r}_{ij}, i\varepsilon_n + i\Omega_m) \tag{65}$$

and $\tilde{\chi}_f(i\varepsilon_m) = \chi_f(i\varepsilon_m)/(g_L\mu_B)^2$, with $\chi_f(i\varepsilon_m)$ the full, single-impurity $f$-spin susceptibility, Eq. (47).

For the renormalization of the total $c$–$f$ vertex for $c$-electrons at the Fermi energy, the contributions $\Lambda^{(d)}_{RKKY}$, $\Lambda^{(d)}_{RKKY}$ must be calculated for real frequencies, $i\Omega \to \Omega + i0$, $i\omega \to \omega + i0$, and for electrons at the Fermi energy, i.e., $\omega = 0$. In this limit, only the real parts of $\Lambda^{(d)}_{RKKY}$, $\Lambda^{(d)}_{RKKY}$ contribute to the vertex renormalization, as seen below. In order to analyze their importance for the RG flow, we will expand them in terms of the small parameter $T_K/D_0$. In the following, the real part of a complex function will be denoted by a prime ' and the imaginary part by a double-prime ".

**Direct contribution.** Since in $\Lambda^{(d)}_{RKKY}$, $\Pi(i\Omega_m)$ and $\tilde{\chi}_f(i\Omega_m)$ appear as a product and $\tilde{\chi}_f(\Omega)$ cuts off the energy transfer $\Omega$ at the scale $T_K \ll \varepsilon_F \approx D_0$, the electron polarization $\Pi(\Omega)$ contributes only in the limit $\Omega \ll \varepsilon_F$ where it is real-valued, as seen in Eq. (45). Using Eq. (45) and Eq. (47), the real part of the direct RKKY-induced vertex contribution reads,

$$\Lambda^{(d)}_{RKKY}{}'(\mathbf{r}_{ij}, \Omega + i0) = JJ_0^2 R(\mathbf{r}_{ij}) AN(0)\,\frac{D_0}{T_K}\,\frac{1}{\sqrt{1+(\Omega/T_K)^2}} \;+\; \mathcal{O}\left(\left(\frac{\Omega}{D_0}\right)^2\right), \tag{66}$$

where

$$R(\mathbf{r}_{ij}) \;=\; \frac{\sin(x) - x\cos(x)}{4x^4}, \qquad\qquad x = 2k_F r \tag{67}$$

is a spatially oscillating function.

**Exchange contribution.** In order to analyze the size of ${\Lambda^{(x)}_{RKKY}}'$ in terms of $T_K/D_0$, it is sufficient to evaluate it for a particle-hole symmetric conduction band and for $\mathbf{r}_{ij} = 0$, since the $T_K/D_0$ dependence is induced by the on-site susceptibility $\tilde{\chi}_f(i\Omega)$. The dependence on $T_K/D_0$ can be changed by the frequency convolution involved in ${\Lambda^{(x)}_{RKKY}}'$, but does not depend on details of the conduction band and distance dependent terms. (The general calculation is possible as well, but considerably more lengthy.) We use the short-hand notation for the momentum-integrated $c$-electron Green function, $G_c(\mathbf{r} = 0, \omega \pm i0) = G(\omega) = G'(\omega) + iG''(\omega)$, and assume a flat density of states $N(\omega)$, with the upper and lower band cutoff symmetric about $\varepsilon_F$, i.e.,

$$G^{R/A\prime\prime}(\omega) = \mp\frac{\pi}{2D_0}\Theta(D_0 - |\omega|) \tag{68}$$

$$G^{R/A\prime}(\omega) = \frac{1}{2D_0}\ln\left|\frac{D_0+\omega}{D_0-\omega}\right| = \frac{\omega}{D_0^2} + \mathcal{O}\left(\left(\frac{\omega}{D_0}\right)\right) . \tag{69}$$

Furthermore, at $T = 0$ the Fermi and Bose distribution functions are, $f(\varepsilon) = -b(\varepsilon) = \Theta(-\varepsilon)$. ${\Lambda^{(x)}_{RKKY}}'(0, 0, \Omega + i0)$ then reads,

$$\begin{aligned}
&{\Lambda^{(x)}_{RKKY}}'(\mathbf{r}_{ij} = 0, \omega = 0 + i0, \Omega + i0) \;=\\
&-JJ_0^2\left\{\int\frac{d\varepsilon}{\pi}\left[f(\varepsilon)G^{A\prime\prime}(\varepsilon)G^{R\prime}(\varepsilon+\Omega) + f(\varepsilon+\Omega)\,G^{A\prime}(\varepsilon)G^{A\prime\prime}(\varepsilon+\Omega)\right]\tilde{\chi}_f^{R\prime}(\varepsilon)\right.\\
&\left.-\int\frac{d\varepsilon}{\pi}\left[f(\varepsilon)\,G^{R\prime}(\varepsilon)G^{R\prime}(\varepsilon+\Omega) - f(\varepsilon+\Omega)G^{A\prime\prime}(\varepsilon)G^{A\prime\prime}(\varepsilon+\Omega)\right]\tilde{\chi}_f^{R\prime\prime}(\varepsilon)\right\} .
\end{aligned} \tag{70}$$

With the above definitions, the four terms in this expression are evaluated in an elementary way, using the substitution $\varepsilon_F/T_K = x = \sinh u$,

$$\begin{aligned}
&\int\frac{d\varepsilon}{\pi}f(\varepsilon)G^{A\prime\prime}(\varepsilon)G^{R\prime}(\varepsilon+\Omega)\tilde{\chi}_f^{R\prime}(\varepsilon)\\
&\qquad= AN(0)\frac{T_K}{D_0}\left[1-\sqrt{1+\left(\frac{D_0}{T_K}\right)^2}+\frac{\Omega}{T_K}\,\mathrm{arsinh}\left(\frac{D_0}{T_K}\right)\right]\\
&\qquad= AN(0)\left[-1+\frac{\Omega}{D_0}\ln\left(\frac{D_0}{T_K}\right)+\mathcal{O}\left(\frac{T_K}{D_0}\right)\right]
\end{aligned} \tag{71}$$

$$\begin{aligned}
&\left|\int\frac{d\varepsilon}{\pi}f(\varepsilon+\Omega)\,G^{A\prime}(\varepsilon)G^{A\prime\prime}(\varepsilon+\Omega)\tilde{\chi}_f^{R\prime}(\varepsilon)\right|\\
&\qquad= AN(0)\frac{T_K}{D_0}\left|\sqrt{1+\left(\frac{\Omega}{T_K}\right)^2}-\sqrt{1+\left(\frac{D_0+\Omega}{T_K}\right)^2}\right|\\
&\qquad\le AN(0)+\mathcal{O}\left(\frac{T_K}{D_0}\right)
\end{aligned} \tag{72}$$

$$\begin{aligned}
&\int\frac{d\varepsilon}{\pi}f(\varepsilon)\,G^{R\prime}(\varepsilon)G^{R\prime}(\varepsilon+\Omega)\tilde{\chi}_f^{R\prime\prime}(\varepsilon)\\
&\qquad= -\frac{4}{\pi^2}AN(0)\left(\frac{1}{2}+\frac{\Omega}{D_0}\right)\ln\left(\frac{D_0}{T_K}\right)+\mathcal{O}\left(\left(\frac{T_K}{D_0}\right)^0\right)
\end{aligned} \tag{73}$$

$$\int \frac{d\varepsilon}{\pi} f(\varepsilon+\Omega) G^{A\prime\prime}(\varepsilon) G^{A\prime\prime}(\varepsilon+\Omega) \tilde{\chi}_f^{R\prime\prime}(\varepsilon)$$
$$= \frac{\pi}{4} AN(0) \left[ -\mathrm{arsinh}\left(\frac{\Omega}{T_K}\right) + \mathrm{arsinh}\left(\min\left(\frac{\Omega}{T_K}, \frac{D_0+\Omega}{T_K}\right)\right)\right]$$
$$\leq \frac{\pi}{4} AN(0) + \mathcal{O}\left(\frac{T_K}{D_0}\right) . \tag{74}$$

Comparing Eqs. (70)–(74) with Eq. (66) shows that all terms of ${\Lambda^{(x)}_{RKKY}}'(\Omega)$ are sub-leading compared to ${\Lambda^{(d)}_{RKKY}}'(\Omega)$ by at least a factor $(T_K/D_0)\ln(T_K/D_0)$ for all transferred energies $\Omega$. Hence, it can be neglected in the RG flow. Combining the results of spin and energy dependence, Eqs. (59), (63), and (66), one obtains the total RKKY-induced $c$–$f$ vertex as,

$$\hat{\gamma}^{(d)}_{RKKY}(\mathbf{r}_{ij}, i\Omega) \;=\; 2\,(1-\delta_{ij})\,\Pi(\mathbf{r}_{ij}, i\Omega)\chi_f(i\Omega)\,\mathbf{S}_i\cdot\mathbf{s}_j \tag{75}$$

or

$$\mathrm{Re}\hat{\gamma}^{(d)}_{RKKY}(\mathbf{r}_{ij}, \Omega+i0) = 2JJ_0^2 AN(0)\,(1-\delta_{ij})R(\mathbf{r}_{ij})\,\frac{D_0}{T_K}\,\frac{1}{\sqrt{1+(\Omega/T_K)^2}}\,\mathbf{S}_i\cdot\mathbf{s}_j. \tag{76}$$

# References


[1] J. Kondo, Prog. Theor. Phys **32**, 37 (1964)

[2] A.C. Hewson: *The Kondo Problem to Heavy Fermions* (Cambridge University Press, 1993)

[3] M.A. Ruderman and C. Kittel, Phys. Rev. **96**, 99 (1954)

[4] T. Kasuya, Prog. Theor. Phys. **16**, 45 (1956)

[5] K. Yosida, Phys. Rev. **106**, 893 (1957)

[6] H. v. Löhneysen, A. Rosch, M. Vojta, and P. Wölfle, Rev. Mod. Phys. **79**, 1015 (2007)

[7] S. Doniach, Physica B+C **91**, 231 (1977)

[8] J.A. Hertz, Phys. Rev. B **14**, 1165 (1976)

[9] T. Moriya: *Spin fluctuations in itinerant electron magnetism* (Springer, Berlin, 1985)

[10] A.J. Millis, Phys. Rev. B **48**, 7183 (1993)

[11] K.Q. Si, S. Rabello and J.L. Smith, Nature **413**, 804 (2001)

[12] P. Coleman, C. Pépin, Q. Si, and R. Ramazashvili, J. Phys.: Condens, Matter **13**, R723 (2001)

[13] T. Senthil, M. Vojta, and S. Sachdev, Phys. Rev. B **69**, 035111 (2004)

[14] P. Wölfle and E. Abrahams, Phys. Rev. B **84**, 041101 (2011)

[15] E. Abrahams, J. Schmalian, and P. Wölfle, Phys. Rev. B **90**, 045105 (2014)

[16] P. Wölfle and E. Abrahams, Phys. Rev. B **93**, 075128 (2016)

[17] A.A. Abrikosov, Physics **2**, 21 (1965)

[18] S.E. Barnes, J. Phys. F **6**, 1375 (1976)

[19] P. Coleman, Phys. Rev. B **29**, 3035 (1984)

[20] J. Kroha and P. Wölfle, Acta Phys. Pol. B **29**, 3781 (1998)

[21] J. Kroha, P. Wölfle, and T.A. Costi, Phys. Rev. Lett. **79**, 216 (1997)

[22] N. Andrei, K. Furuya, and J.H. Lowenstein, Rev. Mod. Phys. **55**, 331 (1983)

[23] R. Bulla, T.A. Costi, and T. Pruschke, Rev. Mod. Phys. **80**, 395 (2008)

[24] P.W. Anderson, J. Phys. C: Solid State Phys. **3**, 2436 (1970)

[25] B.A. Jones, C.M. Varma, and J.W. Wilkins, Phys. Rev. Lett. **61**, 125 (1988)

[26] I. Affleck, A.W.W. Ludwig, and B.A. Jones, Phys. Rev. B **52**, 9528 (1995)

[27] A. Nejati, K. Ballmann, and J. Kroha, Phys. Rev. Lett. **118**, 117204 (2017)

[28] D. Veberič, Computer Phys. Commun. **183**, 2622 (2012)

[29] J. Bork, Y.-H. Zhang, L. Diekhöner, L. Borda, P. Simon, J. Kroha, P. Wahl, and K. Kern, Nat. Phys. **7**, 901 (2011)

[30] N. Néel, R. Berndt, J. Kröger, T.O. Wehling, A.I. Lichtenstein, and M.I. Katsnelson, Phys. Rev. Lett. **107**, 106804 (2011)